

Oral presentation | 10 Spintronics and Magnetism : 10.1 Emerging materials in spintronics and magnetism
(including fabrication and characterization methodologies)

🏠 Fri. Sep 20, 2024 9:00 AM - 11:30 AM JST | Fri. Sep 20, 2024 12:00 AM - 2:30 AM UTC 🏠 D61
(Bandaijima Bldg)

[20a-D61-1~9] 10.1 Emerging materials in spintronics and magnetism (including fabrication and characterization methodologies)

Tomohiro Nozaki(AIST), Kihito Yamada(Tokyo Tech.)

📌 English Presentation 📌 Highlighted Presentation

9:00 AM - 9:15 AM JST | 12:00 AM - 12:15 AM UTC

[20a-D61-1]

Room-temperature flexible manipulation of the quantum-metric structure in a topological chiral antiferromagnet

○Jiahao Han^{1,2}, Tomohiro Uchimura^{1,3}, Yasufumi Araki⁴, Ju-Young Yoon^{1,3}, Yutaro Takeuchi², Yuta Yamane^{1,5}, Shun Kanai^{1,2,3,6,7,8,9}, Junichi Ieda⁴, Hideo Ohno^{1,2,3,8,10}, Shunsuke Fukami^{1,2,3,8,11} (1.RIEC, Tohoku Univ., 2.AIMR, Tohoku Univ., 3.Eng., Tohoku Univ., 4.ASRC, JAEA, 5.FRIS, Tohoku Univ., 6.PRESTO, JST., 7.DEFS, Tohoku Univ., 8.CSIS, Tohoku Univ., 9.QST, 10.CIES, Tohoku Univ., 11.InaRIS)

📌 English Presentation

9:15 AM - 9:30 AM JST | 12:15 AM - 12:30 AM UTC

[20a-D61-2]

Magnetic Phase Diagram of Non-Collinear Antiferromagnet $Mn_{3+x}Sn_{1-x}$ Thin Films

○Katarzyna Gas^{1,2}, Ju-Young Yoon^{3,4}, Yuma Sato^{3,4}, Hiroki Kubota^{3,4}, Jaroslaw Z. Domagala², Piotr Dłuzewski², Yadhu K. Edathumkandy², Yutaro Takeuchi^{3,5,6}, Shun Kanai^{1,3,4,5,7,8,9}, Hideo Ohno^{1,3,5,10}, Maciej Sawicki^{2,3}, Shunsuke Fukami^{1,3,4,5,10} (1.CSIS, Tohoku Univ., 2.Institute of Physics PAS, 3.Laboratory for Nanoelectronics and Spintronics, RIEC, Tohoku Univ., 4.Graduate School of Engineering, Tohoku Univ., 5.WPI-AIMR, Tohoku Univ., 6.ICYS, NIMS, 7.PRESTO, JST, 8.DEFS, Tohoku Univ., 9.NIQST, 10.CIES, Tohoku Univ)

📌 English Presentation

9:30 AM - 9:45 AM JST | 12:30 AM - 12:45 AM UTC

[20a-D61-3]

Improved magnetic properties in CoFeB/MgFeO multilayers with Fe segregated interfaces

○Tomohiro Ichinose¹, Tatsuya Yamamoto¹, Takayuki Nozaki¹, Kay Yakushiji¹, Shingo Tamaru¹, Shinji Yuasa¹ (1.AIST)

📌 English Presentation

9:45 AM - 10:00 AM JST | 12:45 AM - 1:00 AM UTC

[20a-D61-4]

Characterization of spin polarization in ordered Co-based full Heusler $Co_2FeAl_{0.33}Si_{0.67}$ alloy thin films using nano-contact Andreev reflection technique

○(M2)Syunki Kameoka¹, Togo Miyake¹, Jin Ow¹, Yota Takamura¹, Shigeki Nakagawa¹ (1.Tokyo Tech.)

📌 English Presentation

10:00 AM - 10:15 AM JST | 1:00 AM - 1:15 AM UTC

[20a-D61-5]

Large Magnetoresistance and High Spin-Transfer Torque Efficiency of $\text{Co}_2\text{Mn}_x\text{Fe}_{1-x}\text{Ge}$ ($0 \leq x \leq 1$) Heusler Alloy Thin Films Obtained by High-Throughput Compositional Optimization Using Combinatorially Sputtered Composition-Gradient Film

○(PC)Vineet Barwal¹, Hirofumi Suto¹, Ryo Toyama¹, Taisuke Sasaki¹, Yuya Sakuraba¹ (1.NIMS)

◆ English Presentation

10:30 AM - 10:45 AM JST | 1:30 AM - 1:45 AM UTC

[20a-D61-6]

Positive and negative anomalous Nernst coefficients in 2-dimensional layered MnAlGe thin films with large magnetic anisotropy

○(P)Nanhe Kumar Gupta¹, Ryo TOYAMA¹, Benugopal BAIRAGYA¹, Keisuke MASUDA¹, Yuya SAKURABA¹ (1.Research Center for Magnetic and Spintronic Materials, National Institute for Materials Science)

◆ English Presentation

10:45 AM - 11:00 AM JST | 1:45 AM - 2:00 AM UTC

[20a-D61-7]

Direct-Contact Seebeck-Driven Transverse Magneto-Thermoelectric Generation in Magnetic / Thermoelectric Bilayers

○Weinan Zhou¹, Taisuke Sasaki¹, Ken-ichi Uchida¹, Yuya Sakuraba¹ (1.NIMS)

◆ Presentation by Applicant for JSAP Young Scientists Presentation Award ◆ English Presentation

11:00 AM - 11:15 AM JST | 2:00 AM - 2:15 AM UTC

[20a-D61-8]

Anomalous Nernst effect and magnetic structures of Pd/Co multilayers

○(M2)Hayato Kudo¹, Yasuo Takeichi², Shohei Yamashita³, Bowen Qiang¹, Toshio Miyamachi¹, Kanta Ono², Masaki Mizuguchi¹ (1.Nagoya Univ., 2.Osaka Univ., 3.KEK-IMSS)

◆ Presentation by Applicant for JSAP Young Scientists Presentation Award ◆ English Presentation

11:15 AM - 11:30 AM JST | 2:15 AM - 2:30 AM UTC

[20a-D61-9]

Observation of the giant anomalous Nernst effect in the Weyl ferromagnet Co_2MnGa polycrystalline films

○(P)Ryota Uesugi^{1,2}, Tomoya Higo^{1,2,3}, Satoru Nakatsuji^{1,2,3,4,5} (1.Dep. of Phys., Univ. of Tokyo, 2.ISSP, Univ. of Tokyo, 3.CREST, JST, 4.TSQS, Univ. of Tokyo, 5.IQM, JHU)

Room-temperature flexible manipulation of the quantum-metric structure in a topological chiral antiferromagnet

Jiahao Han^{1,2*}, Tomohiro Uchimura^{1,3}, Yasufumi Araki⁴, Ju-Young Yoon^{1,3}, Yutaro Takeuchi², Yuta Yamane^{1,5}, Shun Kanai^{1,2,3,6,7,8,9}, Jun'ichi Ieda⁴, Hideo Ohno^{1,2,3,8,10} & Shunsuke Fukami^{1,2,3,8,10,11}

¹RIEC, Tohoku Univ. ²AIMR, Tohoku Univ. ³Grad School of Eng., Tohoku Univ. ⁴ASRC, JAEA. ⁵FRIS, Tohoku Univ. ⁶PRESTO, JST. ⁷DEFS, Tohoku Univ. ⁸CSIS, Tohoku Univ. ⁹QST. ¹⁰CIES, Tohoku Univ. ¹¹InaRIS. *Presenter email: jiahao.han.c8@tohoku.ac.jp

The quantum metric and Berry curvature are two fundamental and distinct factors that describe the geometry of quantum eigenstates. While the role of the Berry curvature in governing various condensed-matter states has been investigated extensively [1,2], the quantum metric, which was also predicted to induce topological phenomena of equal importance [3], has rarely been studied. Recently, a breakthrough has been made in observing the quantum-metric nonlinear transport in a van der Waals magnet [4,5], but the effect is limited at cryogenic temperature and is tuned by strong magnetic fields of several teslas. In our study [6], we demonstrate room-temperature manipulation of the quantum-metric structure of electronic states through its interplay with the interfacial spin texture in a topological chiral antiferromagnet/heavy metal $\text{Mn}_3\text{Sn}/\text{Pt}$ heterostructure (Fig. 1a), which is manifested in a time-reversal-odd second-order Hall effect (ScHE) (Figs. 1b and 1c). We show the flexibility of controlling the quantum-metric structure with moderate magnetic fields and verify the quantum-metric origin of the observed ScHE by theoretical modeling (Fig. 1c). Our results open the possibility of building applicable nonlinear devices by harnessing the quantum-metric structure of electronic states.

A portion of this work is supported by JSPS Kakenhi Grant Nos. 19H05622, 22K03538, and 22KF0035, MEXT Initiative to Establish Next-Generation Novel Integrated Circuits Centers (X-NICS) Grant No. JPJ011438, and Casio Science and Technology Foundation Grant No. 40-4.

[1] D. Xiao, et al. *Rev. Mod. Phys.* **82**, 1959 (2010). [2] L. Šmejkal, et al. *Nat. Phys.* **14**, 242 (2018). [3] Y. Gao, et al. *Phys. Rev. Lett.* **112**, 166601 (2014). [4] A. Gao, et al. *Science* **381**, 181 (2023). [5] N. Wang, et al. *Nature* **621**, 487 (2023). [6] J. Han, et al. *Nat. Phys.* <https://doi.org/10.1038/s41567-024-02476-2> (2024).

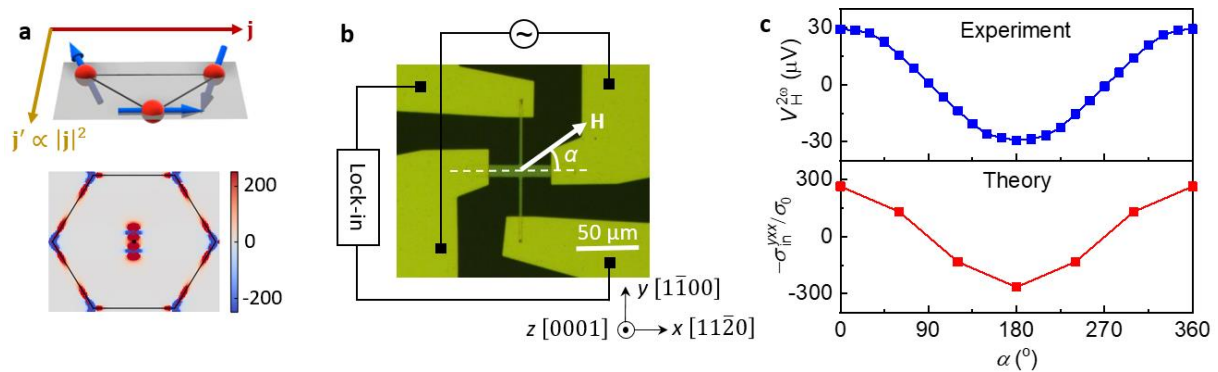


Fig. 1. **a**, Chiral-spin structure with out-of-plane canting in $\text{Mn}_3\text{Sn}/\text{Pt}$ (upper panel), which leads to specific quantum-metric structure (lower panel) as the origin of the ScHE, that is, the Hall current \mathbf{j}' is quadratic to the applied current \mathbf{j} . **b**, Device connected to an alternating current source and a lock-in amplifier to measure the second-harmonic Hall signal to probe the ScHE. A magnetic field \mathbf{H} that can rotate in the sample plane is applied. **c**, Experimental and theoretical ScHE as a function of the applied magnetic field angle. The field strength is fixed at 0.4 T.

Magnetic Phase Diagram of Non-Collinear Antiferromagnet $\text{Mn}_{3+x}\text{Sn}_{1-x}$ Thin Films

°K. Gas^{1,2}, J.-Y. Yoon^{3,4}, Y. Sato^{3,4}, H. Kubota^{3,4}, J. Z. Domagala², P. Dłużewski²,

Y. K. Edathumkandy², Y. Takeuchi^{3,5,6}, S. Kanai^{1,3,4,5,7,8,9}, H. Ohno^{1,3,5,10},

M. Sawicki^{2,3}, and S. Fukami^{1,3,4,5,10}

¹ CSIS, Tohoku Univ., ² Institute of Physics PAS, ³ Laboratory for Nanoelectronics and Spintronics,

RIEC, Tohoku Univ., ⁴ Graduate School of Engineering, Tohoku Univ., ⁵ WPI-AIMR, Tohoku

Univ., ⁶ ICYS, NIMS, ⁷ PRESTO, JST, ⁸ DEFS, Tohoku Univ., ⁹ NIQST, ¹⁰ CIES, Tohoku Univ.

E-mail: gas.katarzyna.a2@tohoku.ac.jp

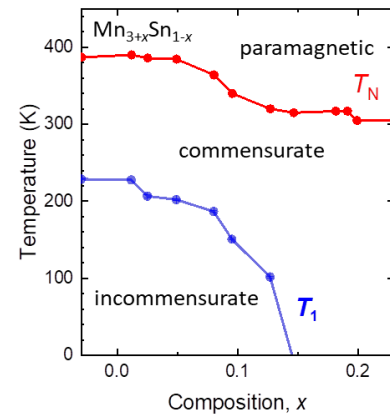
Non-collinear antiferromagnetic $D0_{19}\text{-Mn}_{3+x}\text{Sn}_{1-x}$ exhibits various intriguing properties akin to ferromagnets, such as a large anomalous Hall effect (AHE) arising from the Berry curvature associated with Weyl points [1]. Since its properties are expected to significantly change with the Mn content x through the position of the Fermi level [2] as well as other factors [3,4], the development of systematic knowledge on the role of x in $\text{Mn}_{3+x}\text{Sn}_{1-x}$ on its physical properties is timely and important.

We comprehensively study structural (XRD, TEM), magnetic, and magnetotransport (AHE) [with different temperatures (4 – 400 K)] properties of m -plane-oriented epitaxial $\text{Mn}_{3+x}\text{Sn}_{1-x}$ ($-0.03 \leq x \leq +0.23$) thin layers deposited by magnetron sputtering [5]. This effort allows us, for example, to construct x -dependent magnetic phase diagram (Figure), in which the most profound feature is the disappearance of the transition (at temperature T_1) between an anti-chiral commensurate phase (inverse triangular antiferromagnetic order) to a non-coplanar modulated incommensurate phase [6] for $x \geq +0.15$. This indicates that the inverse triangular antiferromagnetic order exhibiting large AHE can be stabilized down to the liquid He temperatures in thin layers of Mn-rich $\text{Mn}_{3+x}\text{Sn}_{1-x}$. We also find that the Néel temperature (T_N) depends on the Mn composition and correlates with the simultaneous change in the lattice parameter. Our work broadens the understanding of the correlation between the structural and magnetic characteristics of Mn_3Sn thin films towards developing novel devices.

Acknowledgments: This study has been partly supported by TUMUG Support Program from Center for Diversity, Equity, and Inclusion, Tohoku University, and by JSPS Kakenhi 19H05622, 21J23061, 24KJ0432, and 24H00039.

Acknowledgments: This study has been partly supported by TUMUG Support Program from Center for Diversity, Equity, and Inclusion, Tohoku University, and by JSPS Kakenhi 19H05622, 21J23061, 24KJ0432, and 24H00039.

[1] S. Nakatsuji *et al.*, Nature, **527**, 212 (2015). [2] K. Kuroda *et al.*, Nat. Mater., **16**, 1090 (2017). [3] J.-Y. Yoon *et al.*, AIP Advances 11, 065318 (2021). [4] T. Uchimura *et al.*, Appl. Phys. Lett. 120, 172405 (2022). [5] J.-Y. Yoon *et al.*, Appl. Phys. Express, **13**, 013001 (2020). [6] Y. Chen *et al.*, arXiv:2306.07822v3



Improved magnetic properties in CoFeB/MgFeO multilayers with Fe segregated interfaces

AIST¹, [○]Tomohiro Ichinose¹, Tatsuya Yamamoto¹, Takayuki Nozaki¹, Kay Yakushiji¹, Shingo Tamaru¹, Shinji Yuasa¹

E-mail: tomohiro.ichinose@aist.go.jp

Introduction Large perpendicular magnetic anisotropy (PMA) and low magnetic damping (α) in CoFeB/MgO junctions are necessary for magnetoresistive random-access memory applications to realize a long data retention time and low writing energy. Since the PMA and α are sensitive to quality of the CoFeB/MgO interface, various approaches have been attempted to modify the CoFeB/MgO interface. An interesting example is the use of MgFeO instead of MgO; it has been revealed that Fe atoms in the MgFeO layer segregated at the CoFeB/MgFeO interface after annealing. [1] Although the segregated Fe may play a key role on the PMA observed in CoFeB/MgFeO, the chemical and magnetic properties of the segregated Fe remain undefined. In this work, we investigated the properties of Fe segregated from MgFeO and its influence on magnetic properties of CoFeB/MgFeO. [2]

Experiments Co₄₀Fe₄₀B₂₀(*t*_{CoFeB})/MgO(*t*_{MgO})/Mg₄₀Fe₁₀O₅₀(*t*_{MgFeO}) multilayers were deposited by sputtering on Si/SiO₂ wafers with buffer layers. The multilayers were annealed at 300 – 400°C in a vacuum furnace. X-ray photoelectron spectroscopy (XPS) measurements were conducted to evaluate the chemical states of Fe in the multilayers. Magnetic properties of the multilayers were measured with vibrating sample magnetometry and vector network analyzer ferromagnetic resonance.

Results Figure 1 shows Fe-2*p* XPS profiles taken from the multilayer annealed at 300°C. As had been expected, the Fe-2*p* XPS profiles showed that Fe atoms in the CoFeB layer were metallic whereas the MgFeO layer consisted of FeO. In contrast, XPS profiles taken from the MgFeO/Ru interface exhibited peaks corresponding to metallic Fe, which revealed that FeO in the MgFeO layer was reduced to metallic Fe associated with interfacial segregation. As for the magnetic properties, the CoFeB/MgFeO based multilayers exhibited 1.2 times larger PMA compared with CoFeB/MgO multilayers. We also report clear reduction of α in the CoFeB/MgFeO multilayers.

Acknowledgements This presentation was partly based on results obtained from a project, JPNP16007, subsidized by the New Energy and Industrial Technology Development Organization (NEDO).

References [1] K. Yakushiji *et al.*, AIP Adv. **8**, 055905 (2018). [2] T. Ichinose *et al.*, APEX **16**, 113002 (2023).

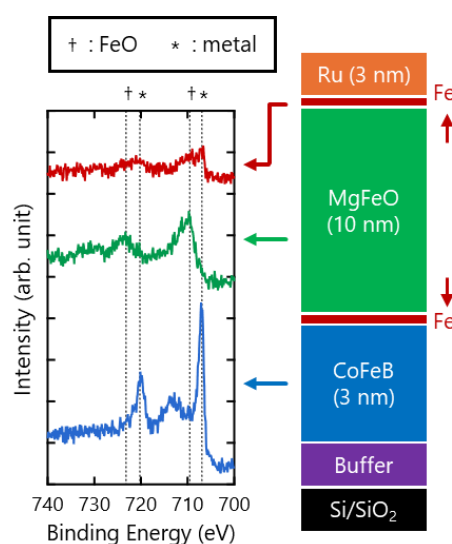


Fig. 1 XPS spectra in CoFeB/MgFeO

ナノコンタクトアンドレーエフ反射を用いた規則相 Co 基フルホイスラ ー合金 $\text{Co}_2\text{FeAl}_{0.33}\text{Si}_{0.67}$ のスピン分極率評価

Characterization of spin polarization in ordered Co-based full Heusler $\text{Co}_2\text{FeAl}_{0.33}\text{Si}_{0.67}$ alloy thin films using nano-contact Andreev reflection technique

東工大¹, [○](M2) 亀岡 俊貴¹, 三宅 玄梧¹, 歐 晋¹, 高村 陽太¹, 中川 茂樹¹

Tokyo Tech¹, [°]S. Kameoka¹, T. Miyake¹, J. Ow¹, Y. Takamura¹, and S. Nakagawa¹

E-mail: kameoka.s.aa@m.titech.ac.jp

The performance of spintronics devices such as magnetoresistive random access memory and highly sensitive sensor, requires the use of ferromagnetic materials with a high spin polarization ratio. The half-metallic nature of Co-based full Heusler $\text{Co}_2\text{FeAl}_{0.33}\text{Si}_{0.67}$ (CFAS) alloys is promising for such devices. The spin polarization of Co-based full Heusler alloys depends on the atomic order in the ordered structures characterized by degree of order^[1] and thus both measurement for the same films is necessary to develop highly spin polarized full-Heusler alloy films. Spin polarization can be accurately measured using nano-contacts Andreev reflection (NCAR) technique^[2] because, the cleanliness contact interface between ferromagnets and superconductors can be kept. In this study, we fabricate nano-contacts junction of CFAS and superconductor Nb by microfabrication, and measured spin polarization of the B2-phase CFAS thin film by NCAR technique.

The $\text{Co}_2\text{FeAl}_{0.33}\text{Si}_{0.67}$ /Nb junctions was fabricated from a structure of MgO(001) substrate/CFAS(70 nm)/Nb(70 nm)/Cr(25 nm)/W(120 nm)/Cr(25 nm), which is formed using a facing target sputtering system. The CFAS layer was deposited at a substrate temperature of 400°C to form the B2 structure. The degree of B2 order was approximately 100%. Figure 1 shows the device structure and measurement configuration. The device was patterned into a 50 nm diameter of pillar using electron beam lithography technique to increase the junction resistance of the CFAS/Nb interface. Additionally, the pillar was headed by etch-back Benzocyclobutene insulating layer by reactive-ion etching to ensure sufficient contact between the pillar and electrodes. The differential conductance dI/dV of the device was measured with lock-in amplifier at 4.2 K in LHe. Figure 2 shows normalized dI/dV as a function of voltage applied to the sample. The residual and parasitic resistances were numerically subtracted. The obtained curve was fitted by an improved Blonder-Tinkham-Klapwijk (BTK) model^[3] to evaluate the spin polarization P . From fitting the spin polarization was determined to be $P = 0.54$ with $\Delta = 3.00$ meV, $Z = 0.15$.

Acknowledgements: We thank ARIM at Tokyo Institute of Technology for help microfabrication system.

Refs: 1. Y. Takamura et al., J. Appl. Phys. **105**, 07B109 (2009). 2. I. Shigeta et al., Appl. Phys. Lett. **112**, 072402 (2018). 3. G. J. Strikers et al., Phys. Rev. B **63**, 104510 (2001).

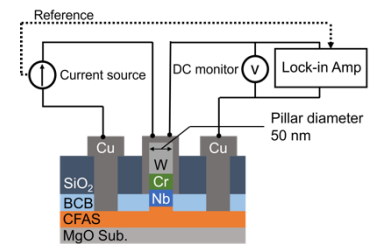


Fig. 1 Device structure and measurement configuration

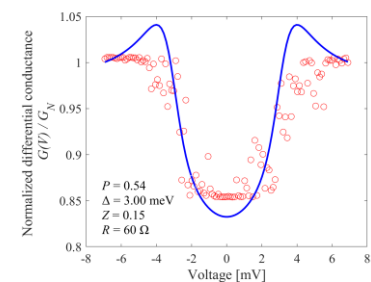


Fig. 2 Normalized differential conductance dI/dV of CFAS/Nb interface at 4.2 K



Large Magnetoresistance and High Spin-Transfer Torque Efficiency of $\text{Co}_2\text{Mn}_x\text{Fe}_{1-x}\text{Ge}$ ($0 \leq x \leq 1$) Heusler Alloy Thin Films Obtained by High-Throughput Compositional Optimization Using Combinatorially Sputtered Composition-Gradient Film

Vineet Barwal, Hirofumi Suto, Ryo Toyama, Taisuke Sasaki and Yuya Sakuraba

Research Center for Magnetic and Spintronic Materials,

National Institute for Materials Science (NIMS), Tsukuba, 305-0047, Japan

E-mail: BARWAL.Vineet@nims.go.jp

Half-metallic ferromagnetic Heusler alloys having high spin polarization have been studied for their potential spintronic applications [1,2]. For certain applications such as current-perpendicular-to-plane giant magnetoresistance (CPP-GMR) read heads, achieving low process temperature, typically below 350°C , is crucial. Moreover, composition tuning is known to be an important factor to enhance the magnetic properties of the Heusler systems, and we developed an experimental method for detailed high-throughput composition optimization using combinatorially sputtered composition-gradient film [3]. In this study, we apply the developed method to $\text{Co}_2\text{Mn}_x\text{Fe}_{1-x}\text{Ge}$ ($0 \leq x \leq 1$) and report high-performance CPP-GMR properties obtained at lower process temperature. Figure (a) shows the deposition process of the composition-gradient thin film. The CPP-GMR stacks shown in Fig. (b), containing composition-gradient $\text{Co}_2\text{Mn}_x\text{Fe}_{1-x}\text{Ge}$ were deposited and processed at different post-annealing (PA) temperatures. Figure (c) shows the position dependence of the atomic concentration in the $\text{Co}_2\text{Mn}_x\text{Fe}_{1-x}\text{Ge}$ film. The XRD measurement revealed the epitaxial and largely single-phase structure throughout the composition range and improved atomic ordering with annealing temperature. The change in MR ratio with Mn content for the stacks annealed at different temperatures is shown in Fig. (d). In the as-deposited sample, the MR ratio exhibited gradual change with Mn content. The CFG side showed lower MR ratio $\sim 2.5\%$ and the CMG side showed slightly higher MR ratio $\sim 5\%$. In the 250°C PA sample, the MR was greatly enhanced and exhibited the following clear composition dependence. The MR ratio was $\sim 22\%$ at $x = 0$, increased gradually with increasing x , and showed a maximum MR ratio of $\sim 35\%$ at around $x = 0.85$. Then it decreased to the CMG side. In the 350°C PA sample, MR was further enhanced with maximum MR ratio of $\sim 45\%$ in the broad x range. The trend of MR ratio versus x changed from the case of 250°C PA sample. First, it increased in the x range of 0-0.2, stayed almost constant in broad x range of 0.2-0.7, and then abruptly decreased near the CMG side. The optimal composition for the highest MR changed with annealing temperature because of the stability of the GMR stack being higher in the lower x range. We achieved record high MR for the CPP-GMR devices at relatively low annealing temperature of 250°C by the present composition optimization method. The results provide comprehensive guidance on the composition optimization to obtain large MR ratio and high STT efficiency in the CPP-GMR devices employing $\text{Co}_2\text{Mn}_x\text{Fe}_{1-x}\text{Ge}$ at relatively low process temperature. In the presentation, the results related to high STT efficiency will also be discussed. The authors acknowledge the support from Advanced Storage Research Consortium (ASRC) and JST CREST Grant No. JPMJCR21O1.

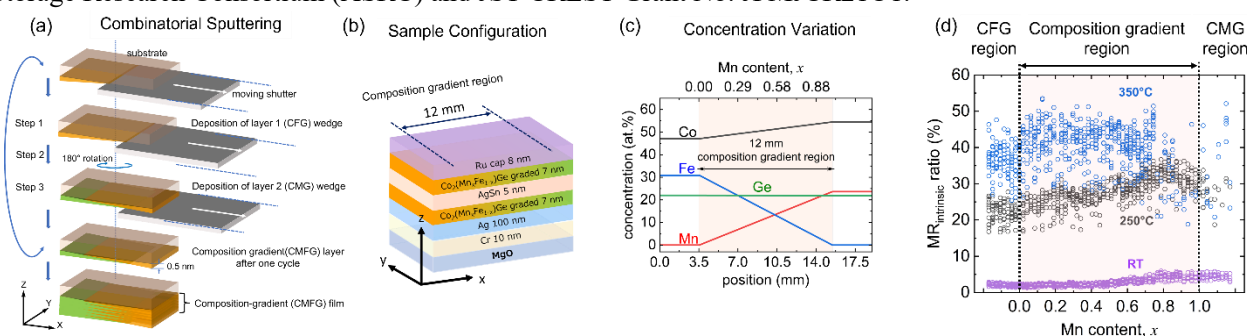


Figure: (a) Schematic showing the Combinatorial sputtering process. (b) Configuration for the CPP-GMR stack. Post-annealing was done after the deposition of the upper $\text{Co}_2\text{Mn}_x\text{Fe}_{1-x}\text{Ge}$ layer. (c) Variation of atomic concentration in $\text{Co}_2\text{Mn}_x\text{Fe}_{1-x}\text{Ge}$ composition-gradient film. (d) Change in intrinsic MR ratio with Mn content for the CPP-GMR stack with different annealing temperatures.

References

- [1] T. Nakatani, Z. Gao, and K. Hono, MRS Bull. **43**, 106 (2018).
- [2] T. Kubota, Z. Wen, and K. Takamashi, J. Magn. Mater. **492**, 165667 (2019).
- [3] V. Barwal, H. Suto, T. Taniguchi, and Y. Sakuraba, Sci. Technol. Adv. Mater. Methods **3**, 1 (2023).

Positive and negative anomalous Nernst coefficients in 2 - dimensional layered MnAlGe thin films with large magnetic anisotropy

Nanhe Kumar Gupta¹, R. Toyama¹, B. Bairagya¹, K. Masuda¹ and Y. Sakuraba¹

¹Research Center for Magnetic and Spintronic Materials, National Institute for Materials Science (NIMS),

Tsukuba, 305-0047, Japan

E-mail: GUPTA.Nanhekumar@nims.go.jp

Ferromagnets with remarkable transverse transport properties, low saturation magnetization (M_s), and high uniaxial magneto crystalline anisotropy constant (K_u) are attracting attention for application in thermopower devices [1]. MnAlGe is an emerging material class with various interesting properties owing to a layered topological nodal line. Reports on the temperature dependence anomalous Nernst effect (ANE) and anomalous Nernst conductivity (α_{xy}) in this class of materials are, however, very limited [2-3]. In this study, the ANE in MnAlGe film with a pseudo-two-dimensional structure consisting of Mn and Al-Ge layers was investigated over a wide temperature range (10-400 K). Using sputtering, the $\text{Mn}_{1.02}\text{Al}_{0.93}\text{Ge}_{1.04}$ films were grown epitaxially on single-crystal MgO (001) substrates. The M_s was as low as ~ 260 emu/cc and K_u was as high as ~ 6 Merg/cc. The relatively large anomalous Hall angles of ~ 0.032 (0.02) were obtained in the film at 25 (300) K, which could be attributed to layered topological nodal lines in these materials [2]. The observed anomalous Nernst coefficient (S_{ANE}) of ~ 2.0 (-0.5) $\mu\text{V/K}$ [Fig. 1(a)] and anomalous Hall conductivity (σ^A_{xy}) of 656 (138) S/cm [Fig. 1(b)] yielded α_{xy} of 4.5 (-0.17) A/(m K) at 25 (300) K [Fig. 1(b)], respectively. The sign change in S_{ANE} occurs at 125 K, which was not observed in the anomalous Hall effect of the film. We performed the first-principles calculation of α_{xy} at 300K and found α_{xy} shows the negative sign which agrees with the experimental observation.

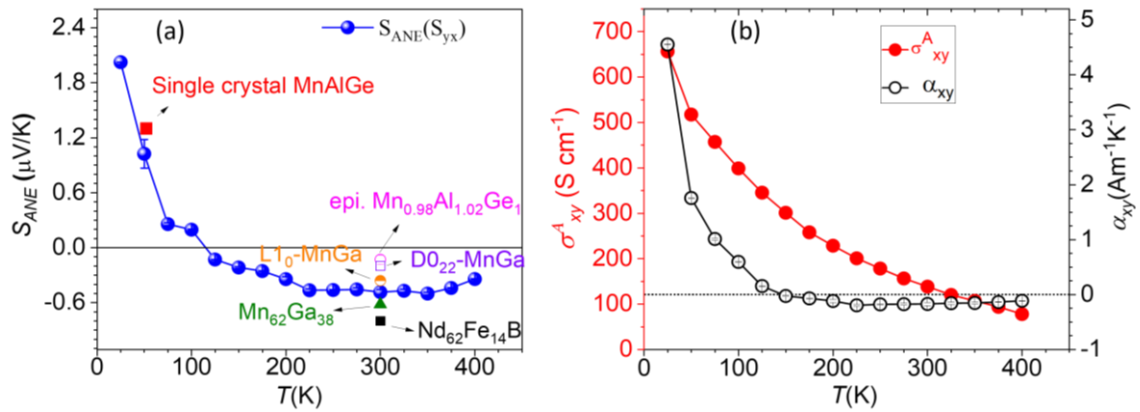


Figure: (a), (b) Temperature dependence of anomalous Nernst coefficient (S_{ANE}), anomalous Nernst conductivity (α_{xy}), anomalous Hall conductivity (σ^A_{xy}) and comparison with existing S_{ANE} values for different material in the literature [4] at 300K.

[1] K. Uchida, *et.al.* Appl. Phys. Lett. 118, 140504 (2021).

[2] S. N. Guin, *et. al.* Adv. Mater. 33,2006301 (2021).

[3] K. Ito, *et. al.* Phys. Rev. Applied 21, 054012 (2024).

[4] W. Zhou, *et.al.* Appl. Phys. Lett. 118, 152406 (2021).

Direct-Contact Seebeck-Driven Transverse Magneto-Thermoelectric Generation in Magnetic / Thermoelectric Bilayers

NIMS, °Weinan Zhou, Taisuke Sasaki, Ken-ichi Uchida, Yuya Sakuraba

E-mail: ZHOU.Weinan@nims.go.jp

Transverse thermoelectric generation can convert temperature gradient (∇T) in one direction into electric field (\mathbf{E}) perpendicular to that direction, where the anomalous Nernst effect (ANE) observed in magnetic materials is a well-known example. The orthogonal relationship between ∇T and \mathbf{E} allows the thermoelectric module to have a simple two-dimensional structure made of connecting wires on a surface, which is beneficial for better flexibility and scalability while avoiding some challenging problems facing modules based on the Seebeck effect (SE) [1]. However, the transverse thermopower of ANE is still small compared to the longitudinal thermopower of SE of thermoelectric materials, and further enhancement is strongly required for applications. Recently, significant enhancement of transverse thermopower is observed in closed circuits consisting of magnetic and thermoelectric materials, which is referred to as the Seebeck-driven transverse magneto-thermoelectric generation (STTG). The strong SE of the thermoelectric material generates a large longitudinal charge current in the magnetic material, which is then converted to the transverse direction by its anomalous Hall effect, leading to a giant transverse thermopower [2]. However, the formation of a closed circuit requires electrical connection only at the two ends along the direction of ∇T but insulation in between, which could be a complicated structure to fabricate and hinder its wide adoption. In this study, we realize STTG in the simplest way to combine magnetic and thermoelectric materials, namely, by stacking a magnetic layer and a thermoelectric layer together to form a bilayer. Different from the closed circuit used in previous studies of STTG, the magnetic and thermoelectric layers are in direct contact over the entire interface. We model the magnetic / thermoelectric bilayer and derive the expression for its transverse thermopower, which varies with changing layer thicknesses and peaks at a much larger value under an optimal thickness ratio (Fig. 1). We reproduced this behavior in the experiment. We measured the transport properties of a serial of samples, which are prepared by depositing Fe-Ga alloy thin films of various thicknesses onto n -type Si substrates. Here, the Fe-Ga film is the magnetic material, while the n -type Si is the thermoelectric material. The predicted tendency of transverse thermopower is nicely reproduced by the measured results as shown in Fig. 1. The value obtained from the sample with optimized layered structures reaches $15.2 \pm 0.4 \mu\text{V K}^{-1}$, which is a fivefold increase from that of Fe-Ga alloy and much larger than the current room temperature record observed in Weyl semimetal Co_2MnGa . Our findings highlight the potential in combining magnetic and thermoelectric materials for transverse thermoelectric applications [3].

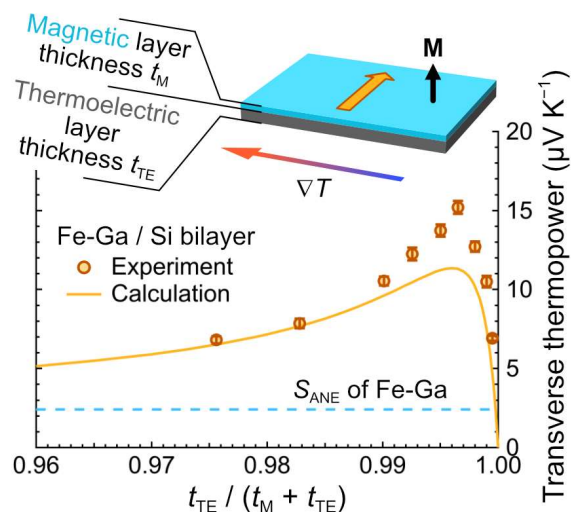


Fig. 1 Transverse thermopower of Fe-Ga / Si bilayer as a function of thickness ratio between the magnetic layer thickness (t_M) and the total thickness of bilayer ($t_M + t_{TE}$).

[1] K. Uchida *et al.*, *Appl. Phys. Lett.* **118**, 140504 (2021).

[2] W. Zhou *et al.*, *Nat. Mater.* **20**, 463 (2021).

[3] W. Zhou *et al.*, *Adv. Sci.* **11**, 2308543 (2024).

Anomalous Nernst effect and magnetic structures of Pd/Co multilayers

(M2)^o Hayato Kudo¹, Yasuo Takeichi², Shohei Yamashita³,

Bowen Qiang¹, Toshio Miyamachi¹, Kanta Ono², Masaki Mizuguchi¹

Nagoya Univ.¹, Osaka Univ.², KEK-IMSS³

E-mail: mizuguchi.masaki@material.nagoya-u.ac.jp

Abstract

In recent years, the anomalous Nernst effect (ANE) has been attracting attention because of its application to a sustainable energy source. The ANE, the thermal counterpart of the AHE, is phenomenon that converts heat flow into transverse voltage in magnetic materials and therefore magnetic structures and their dynamics are thought to be greatly important. Actually, there have been many interesting reports such as observation of topological contributions to the AHE and ANE^[1] with chiral magnetic structures like magnetic skyrmions and prediction of transverse magnon-drag effect^[2]. We have presented the ANE in chiral magnetic samples and discussed their magnetic structures and the ANE. In this talk, we focus on the magnetic structure at each point in a magnetic hysteresis loop and investigate relationship between their magnetic structures and the AHE and ANE.

Experimental method

[Pd (t_{Pd} nm) / Co (0.2 nm)]₁₅ (t_{Pd} = 1.0, 1.5, 2.0, 2.5, and 3.0) films were grown onto thermally oxidized Si substrates by using magnetron sputtering at room temperature. After the growth, we applied some optional magnetic fields to films and characterized their magnetic structures by magnetic force microscopy (MFM). Then, we performed the AHE and ANE measurements by Physical Properties Measurement System (PPMS). We also conducted Scanning Transmission X-ray Microscopy (STXM) measurements for a [Pd (1.0 nm) / Co (0.2 nm)]₅₀ film grown on a SiN membrane and observed its magnetic structures.

Result

Figure 1 shows a STXM image of a [Pd (1.0 nm) / Co (0.2 nm)]₅₀ film. As shown in the figure, the film exhibits an obvious particle-like magnetic structure and this looks same as that observed by MFM. In our presentation, we will focus on the evolution of magnetic structures with magnetic field and discuss relation with the AHE and ANE.

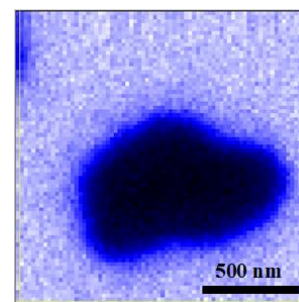


Fig 1 STXM image of [Pd (1.0 nm) / Co (0.2 nm)]₅₀ film.

Reference

- [1] Max Hirschberger *et al.*, Phys. Rev. Lett. **125**, 076602(2020).
- [2] Jun-ichiro Ohe *et al.*, Appl. Phys. Lett. **117**, 062404(2020).

